26th International Congress on Modelling and Simulation, Adelaide, SA, Australia, 30 Nov–4 Dec 2025
mssanz.org.au/modsim2025

Design validation and verification for non-intrusive flight test instrumentation (NIFTI) using Model-Based Systems Engineering (MBSE)

K Pattarakunnan [a], S Bruce [a], E Balaburov [a], and S Mancarella [a]

[a] *MEMKO Pty Ltd, L28/303 Collins Street, Melbourne, VIC 3000, Australia*
Email: bright@memko.com.au

Abstract: Model-Based Systems Engineering (MBSE) combined with Multiphysics simulation offers an effective integrated workflow that can accelerate validation and verification by leveraging Systems Modelling Language (SysML) and reduce the need for physical prototyping through accurate what-if simulations. This study demonstrates how such a workflow can be established using CATIA Magic and Dymola in the context of a novel Non-Intrusive Flight Test Instrumentation or NIFTI developed by MEMKO. As an electronic device, NIFTI must meet two key requirements: (i) it shall supply less than 10 mA of electrical current to a connected strain gauge, and (ii) its battery shall retain at least 80% State of Health (SOH) (i.e. 80% of nominal capacity) after 500 full charge-discharge cycles. To verify these requirements, Dymola models of strain gauge behaviour and battery ageing were developed and validated, and they were then exported as Functional Mock-up Units (FMUs). The FMUs were imported into CATIA Magic to perform sequential simulations using SysML. That is, the strain gauge simulation provided predicted electrical current as an input to the battery ageing simulation which in turn predicted SOH. The predicted values were verified against the defined key requirements. Requirements verification for multiple configurations (of various strain gauge electrical properties and bridge configurations generated using Design of Experiments (DOE)) was also demonstrated through approximately 900 sequential simulations.

Keywords: *Model Based Systems Engineering, Systems Modelling Language (SysML), Multiphysics Simulation, Integrated Simulation Workflow, Digital Engineering*

1. INTRODUCTION

Systems Engineering (SE) is an engineering discipline focused on designing, developing, and managing complex systems by integrating knowledge from multiple domains. While organisations may adapt their own frameworks and terminology, the International Council on Systems Engineering (INCOSE) broadly defines SE as "a transdisciplinary and integrative approach to enable the successful realisation, use, and retirement of engineered systems, using systems principles and concepts, and scientific, technological, and management methods" (INCOSE 2025).

Model-Based Systems Engineering (MBSE) extends traditional SE by using models to support system requirements, design, analysis, verification, and validation from the conceptual phase through to later life cycle stages. One of its key advantages is the ability to maintain a singular authoritative source for each datum, and this is commonly referred to as a Single Source of Truth which ensures consistency, traceability, and avoids duplication. MBSE models can be developed using tools such as CATIA Magic, which supports systems architecture modelling and integration with simulation environments through Functional Mock-up Units (FMUs). The combination of these technologies and their integrated utilisation can be referred to as Digital Engineering.

This paper presents an integrated simulation workflow demonstrating how CATIA Magic was used in conjunction with FMUs developed in the Modelica-based simulation environment Dymola. Dymola enables high-fidelity, multi-physics simulations (Pattarakunnan et al. 2025) such as electrical systems modelling, which forms a core element of Non-Intrusive Flight Test Instrumentation (NIFTI). Design of Experiments (DOE) studies conducted on multiple NIFTI configurations using Dymola FMUs provide performance data to validate and verify the requirements defined in CATIA Magic. As NIFTI is a novel system with limited historical performance data, this approach enables early, reliable design validation and verification without reliance on extensive physical prototyping. It must also be noted that although this work demonstrates the use of CATIA Magic on a small-scale product, the tool has also been applied successfully to much larger and more complex systems such as a lunar base (Boyer et al. 2025).

2. NIFTI BACKGROUND AND REQUIREMENTS

Designed by MEMKO, NIFTI is a small, aircraft independent, wireless sensing system that collects environmental and structural data using sensor nodes adhesively mounted on to an aircraft's structure (Mancarella and Penhall 2025). It has been developed in close collaboration with the Royal Australian Air Force (RAAF) Air Warfare Centre (AWC) and has been flight qualified on a number of aircraft.

There are two variants of NIFTI Sensor Nodes. The first being NIFTI Accelerometer Sensor Node which features high-resolution sensors that measure tri-axial linear acceleration and temperature at a data sampling rate up to 4000 Hz. The second is the NIFTI Strain Gauge Sensor Node ("NIFTI Node") which will be used as a demonstrator in this work. It captures high resolution three-channel measurement data from external sensors (e.g. strain gauges) connected through the External Sensor Port at a sampling rate up to 2000 Hz. To prevent damage, usage of this port must be controlled. A key requirement is that it provides a 2.5 V excitation voltage to connected sensors, and they must not draw more than 10 mA of current from the NIFTI Node (Requirement #1).

Moreover, NIFTI is powered solely by a Lithium-ion Polymer (LiPo) battery and therefore it is crucial to ensure the battery meets the lifecycle requirement. That is, the battery must be able to retain at least 80% of its nominal energy capacity (i.e. 80% State of Health (SOH)) after 500 cycles of full charge and discharge (Requirement #2). Both key requirements are summarised in Table 1.

Table 1 The key requirements to be modelled and managed within CATIA Magic

ID	Name	Content
1	Current Drawn Requirement	Predicted current drawn should be less than 10 mA.
2	Battery SOH Requirement	Predicted Battery SOH should be at least 80%.

3. METHODOLOGIES, RESULTS AND DISCUSSION

This section is divided into two subsections outlining the modelling methodologies used in Dymola (Section 3.1) and CATIA Magic (Section 3.2). The process begins with modelling the strain gauge circuit (Section 3.1.1) and battery ageing (Section 3.1.2) behaviours in Dymola to generate FMUs. These FMUs are then imported into CATIA Magic as Systems Modelling Language (SysML) Block elements. Sequential simulations are performed in CATIA Magic through FMUs, starting with hundreds of strain gauge circuit configurations defined using DOE to predict and calculate current draw from the strain gauge circuit. This is followed by battery ageing simulations that predict and calculate SOH using the previously calculated current draw as the battery discharge rate. The results obtained are then verified against the key requirements listed in Table 1.

3.1. Dymola

3.1.1. Strain Gauge Circuit

A strain gauge circuit is typically represented by a Wheatstone bridge consisting of four resistors, some fixed and others variable depending on the bridge type. In the Quarter Wheatstone bridge used here to validate the simulation, one resistor (R_1) is variable and represents the strain gauge, while the other three (R_2, R_3, R_4) are fixed. A typical Quarter Wheatstone bridge is shown in Figure 1a, and its connection to a single channel of the NIFTI Node is shown in Figure 1b. When no force is applied, R_1 matches the resistance of the other arms (1,000 Ω), producing a balanced bridge with a sense voltage (V_{Sense}) of 0 V. However, a small initial current (I_{Draw}) is still drawn from the NIFTI Node.

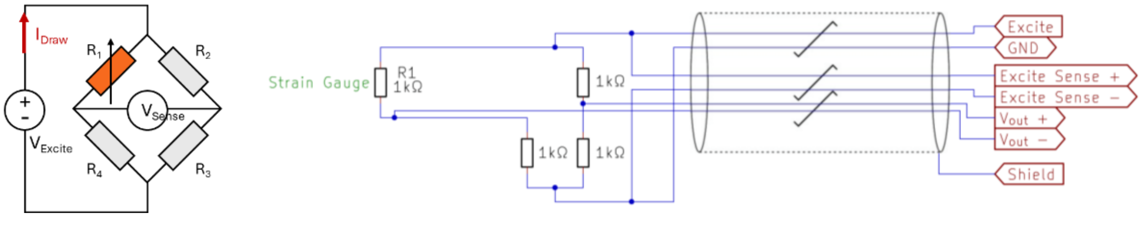

(a) (b)

Figure 1 Quarter Wheatstone bridge showing: (a) Typical circuit and (b) The circuit compatible with NIFTI Node (MEMKO 2025).

Using Dymola's object-oriented modelling approach and standard Modelica Electrical library, the Quarter Wheatstone bridge is modelled according to its real-world physical connections as illustrated in Figure 1b. The bridge is excited by the NIFTI Node with a 2.5 V excitation voltage (V_{Excite}). Under applied structural load or strain (ε), R_1 changes resistance proportionally according to Equation (1):

$$R_1 = R_{1,Initial} + \left(\varepsilon \times GF \times R_{1,Initial}\right) \quad (1)$$

where GF is the gauge factor and $R_{1,Initial}$ is the initial strain gauge resistance. This change in resistance produces corresponding variations in the simulated V_{Sense} and I_{Draw}. Simulated V_{Sense} is validated against experimental measurements while simulated I_{Draw} is later used to verify Requirement #1 in CATIA Magic. The model also includes an optional limiting resistor (R_{lim}) that can be adjusted to influence simulated results, particularly I_{Draw}. This capability becomes useful when conducting DOE in CATIA Magic. The electrical properties required for accurate modelling are summarised in Table 2, and the complete Wheatstone bridge model is shown in Figure 2.

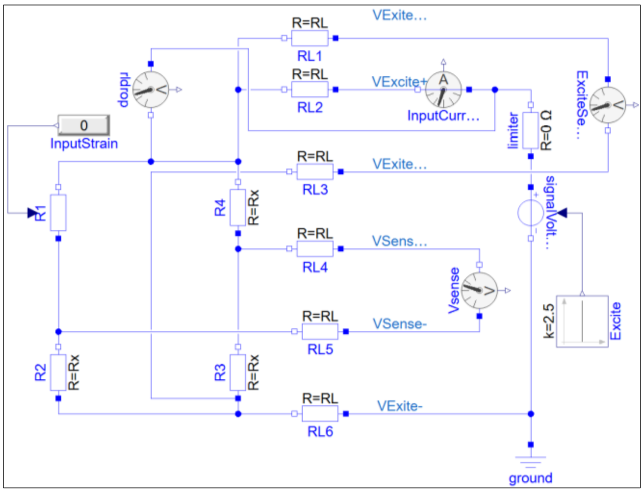

Figure 2 Dymola model of Quarter Wheatstone bridge to a single channel of the NIFTI Node

Figure 3 shows a representative comparison (from six datasets) of experimental and simulated V_{Sense}. The simulated results closely align with experimental measurements, with an average error of less than 10% across all datasets. The observed errors are expected and primarily attributed to three factors: (1) physical tolerances in strain gauges and bridge resistors, meaning actual resistor values deviate slightly from the nominal 1,000 Ω; (2) assumptions made in deriving R_L and GF; and (3) small variations (i.e. noise) in the supplied V_{Excite} in practice, compared to the constant V_{Excite} assumed in simulation. The close agreement validates the simulation model, which can be further refined and adapted to other Wheatstone bridge configurations.

A full Wheatstone bridge model consisting of four variable resistors was developed based on the Quarter Wheatstone bridge model to explore an alternative configuration for verifying compatible strain gauges in CATIA Magic. The electrical properties for the full bridge are identical to those used for the quarter bridge (Table 2). The main difference is that under applied load, R_1 and R_3 vary according to Equation (1), while R_2 and R_4 vary according to Equation (2). Both the Quarter and Full Wheatstone bridge models connected to a single channel of the NIFTI Node can be extended to three-channel configurations by duplication. These can then be exported from Dymola as FMUs for subsequent import and use within CATIA Magic.

$$R_2 = R_{2,Initial} - \left(\varepsilon \times GF \times R_{2,Initial}\right) \qquad (2)$$

Table 2 Key electrical properties used for Wheatstone bridge simulation

Parameter	Value	Unit
Excitation Voltage, V_{Excite}	2.5	V
Initial Strain Gauge Resistance, $R_{1,Initial}$	1,000	Ω
Bridge Resistance, $R_2 = R_3 = R_4$	1,000	Ω
Line Resistance, R_L*	0.778	Ω
Limiting Resistor, R_{Lim}*	0	Ω
Gauge Factor, GF	2.13	-

* *Obtained experimentally*

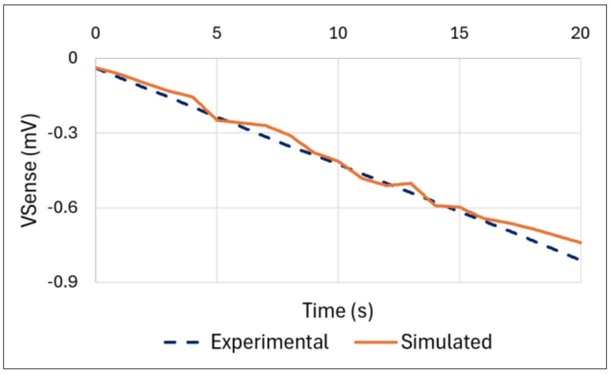

Figure 3 A representative comparison of experimental and simulated V_{Sense}.

3.1.2. Battery Ageing

The ageing simulation of NIFTI LiPo battery (LP672030 380mAh 3.7V – (LiPol Battery 2019)) was developed in Dymola using the Dassault Systèmes Battery Library. While the model can account for holistic ageing effects (Schmalstieg et al. 2014) including thermal behaviour, calendar ageing, and cycling ageing, this study focuses solely on cycling ageing. The simulation replicates the experimental charge-discharge characteristics of the battery with both experimental and simulated current profiles shown in Figure 4a. Charging and discharging of a single battery cycle follow these steps:

1. Constant Current (CC) Charging – The battery is charged at 400 mAh^{-1} until reaching the maximum recommended LiPo battery voltage of 4.2 V.
2. Constant Voltage (CV) Charging – Voltage is held at 4.2 V while the charging current is gradually reduced.
3. Resting Period – The battery rests for 30 minutes after CV charging before discharging.
4. CC Discharge – The battery is discharged at 200 mAh^{-1} until reaching the minimum recommended LiPo battery voltage of 3.2 V.

Following these procedures, experimental and simulated voltage profiles for both charging and discharging were obtained (Figure 4b). The strong agreement between experimental and simulated results confirms the validity of the generated model for a single battery cycle.

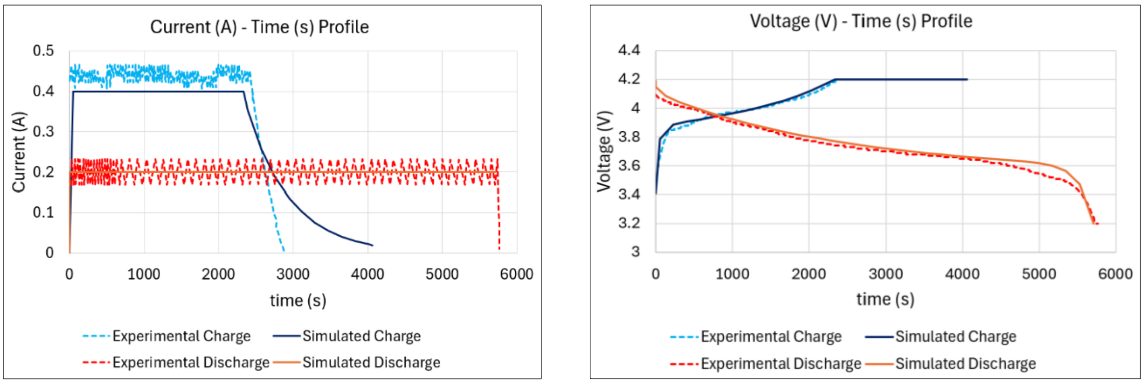

(a) (b)

Figure 4 Experimental and simulated comparison of (a) Current profiles and (b) Voltage profiles

The model was then extended to simulate hundreds of cycles to predict the point at which the battery SOH declines to 80%. Charging and discharging were performed following the same procedures continuously until the target SOH was reached. The simulation predicted that 670 cycles are required to reach 80% SOH. While this is optimistic compared to the manufacturer's specified 500 cycles (LiPol Battery 2019), the result is within a reasonable range and demonstrates the model's capability to produce realistic lifecycle predictions. To align with the manufacturer's specification, the model was adjusted to stop the simulation at 500 cycles, with the SOH at this point reported for use in verifying Requirement #2 in CATIA Magic. At this stage, the battery ageing model is validated and exported from Dymola as an FMU for further integration into CATIA Magic.

3.2. CATIA Magic

CATIA Magic was used to construct a logical architecture of NIFTI Node. This study presents a simplified MBSE model of NIFTI consisting of two main components including Strain Gauge and Battery Management and Monitoring with each represented as a SysML block in CATIA Magic as shown in Figure 5.

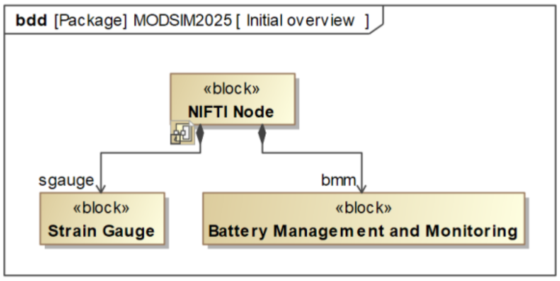

Figure 5 Simplified NIFTI logical architecture

The Strain Gauge block contains value properties as shown in Figure 6a. It is associated with two variants being the Quarter Wheatstone Bridge FMU and the Full Wheatstone Bridge FMU which are linked through a generalisation relationship. In SysML, "generalisation" means that the variants inherit all properties including value properties from the parent block. This approach avoids duplication and ensures that any changes to the parent block's properties are automatically reflected in all variants. To map FMU parameters to CATIA Magic value properties, a Block Definition Diagram (BDD) is used to bind simulation inputs and outputs (defined as SysML Ports) to the Value Properties. Similar approaches were applied to the Battery Management and Monitoring block as shown in Figure 6b.

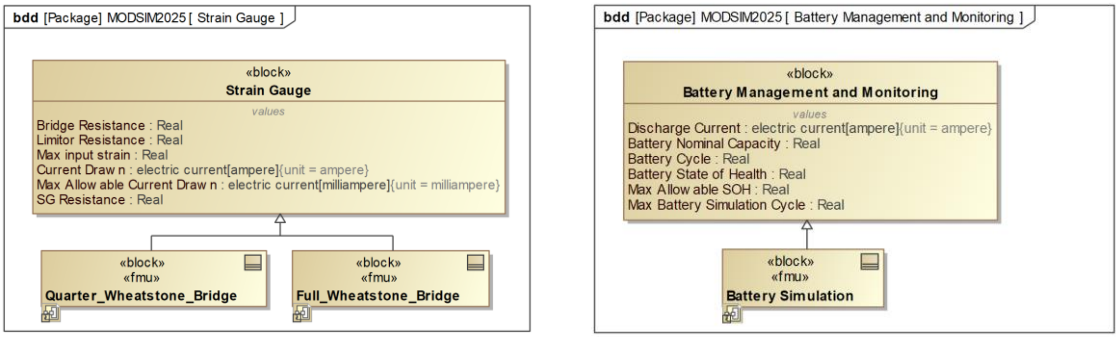

(a) (b)

Figure 6 (a) Strain Gauge block and (b) Battery Management and Monitoring block with generalisation relationships to their variants

At this stage, the simulations can be executed; however, they would run independently and simultaneously. The aim is to have the strain gauge simulation run first to calculate I_{Draw} which is then sequentially used as the discharge current input for the battery simulation. This sequencing can be achieved by constructing a SysML Internal Block Diagram (IBD) at the NIFTI Node block, as it oversees its components and can collect and route data between them. In contrast, the Strain Gauge and Battery Management and Monitoring blocks should not manage data transfer between one another. Figure 7 illustrates an IBD showing this data flow.

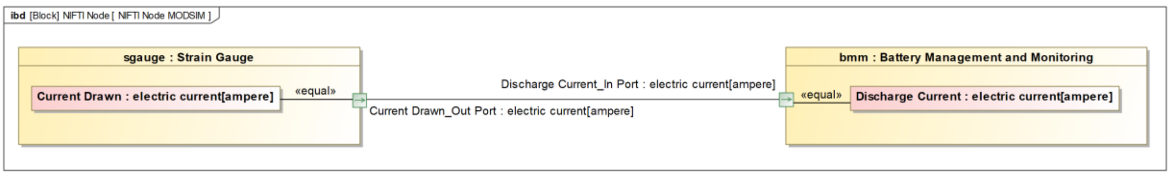

Figure 7 IBD showing I_{Draw} output from the strain gauge simulation used as the discharge current input for the battery simulation

The necessary simulation results including I_{Draw} and SOH were obtained and must now be verified against the requirements in Table 1. For this purpose, a Requirement Verification block consisting of the NIFTI Node block was created along with the relevant requirements and constraints to complete the NIFTI MBSE model as shown in Figure 8. The "satisfy" relationships indicate that I_{Draw} must meet Requirement #1 and SOH must meet Requirement #2. These requirements are further refined using "refine" relationships with constraint blocks implementing the applicable formulas. Moreover, this setup automatically flags simulation results in green when requirements are met and in red when they are not as later illustrated in Figure 9.

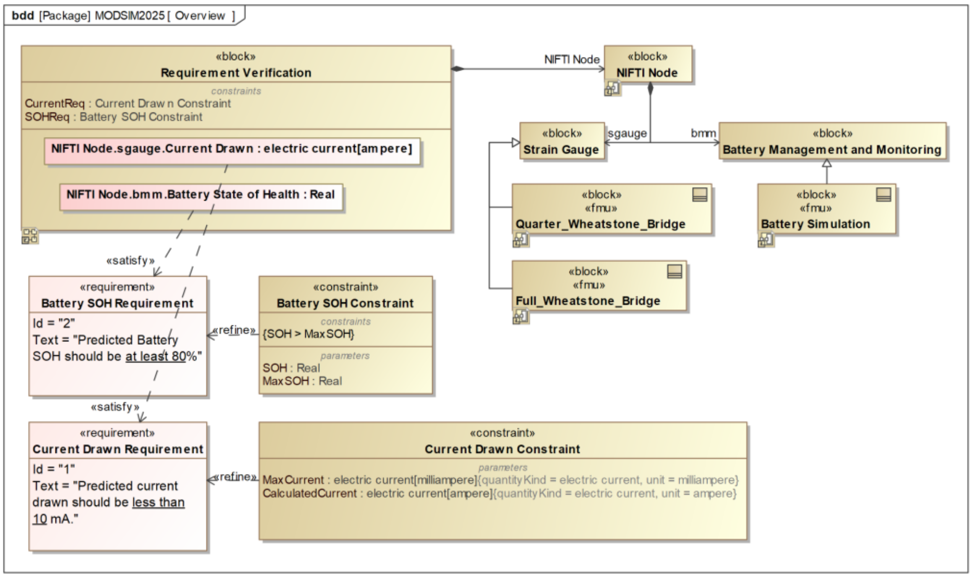

Figure 8 Overview of the complete NIFTI MBSE model

In CATIA Magic, one simulation run is considered as one instance. To execute multiple simulations with different value properties and FMU variants, an instance table can be used to define the simulation inputs and FMU selections. In this study, design configurations were manually generated using Excel using a Full Factorial DOE technique by combining the following variants:

- 21 variants of Strain Gauge Resistance (assumed equal to Bridge Resistance) from 500 to 1500 Ω
- 11 variants of Limiting Resistor from 0 to 500 Ω
- 2 variants of Maximum Input Strain of ±0.05
- 2 Wheatstone Bridge types (Full and Quarter)

This was not performed in CATIA Magic because it lacks built-in DOE support. While CATIA Magic offers similar functionality such as trade study analysis, it often requires advanced users to develop macros and scripts. This makes the approach impractical for smaller projects, including this study, due to the time required. A total of 924 design configurations was produced and imported to CATIA Magic for analysis, with partial simulation results shown in Figure 9. This integrated simulation approach proved effective for evaluating multiple configurations while verifying and validating results against the requirements. It enabled virtual design exploration by leveraging the strengths of both tools including Dymola and CATIA Magic.

4. CONCLUSION

This study demonstrates that an integrated simulation workflow combining Multiphysics simulations and MBSE can be achieved using Dymola and CATIA Magic. Object-oriented modelling in Dymola accurately predicted the electrical behaviour of strain gauge circuits such as the Quarter Wheatstone Bridge and extended to the Full Wheatstone Bridge. Dymola's specialised Battery library enabled modelling of more complex phenomena including battery cycling and ageing. While simulated results did not perfectly match experimental data, they were within a reliable range for early-stage design. By exporting FMUs, Dymola provided the key link to CATIA Magic which is used to model and create MBSE systems, configure FMU variants, and implement requirements and constraints for verification and validation. Hundreds of design configurations were imported and simulated, demonstrating the workflow's ability to reduce prototyping needs, accelerate verification, and provide early confidence in meeting product requirements. To improve the workflow's seamlessness, CATIA Magic-Dymola integration (e.g. via connectors) could be explored in addition to FMU import/export. DOE-capable analysers such as 3DExperience Process Composer could also be integrated to enable DOE functionality currently limited in CATIA Magic. This would enable DOE methods such as

Fractional Factorial Design, Latin Hypercube, and Box-Behnken, as well as process automation and optimisation through algorithms like Hooke–Jeeves, Multi-Objective Particle Swarm, and Downhill Simplex. However, trade-offs should be considered for small-scale projects, where time constraints and required expertise may outweigh the benefits.

Verification Status: Pass Fail

#	NIFTI Node.sgauge : Strain Gauge	NIFTI Node.sgauge. Bridge Resistance : Real	NIFTI Node.sgauge. SG Resistance : Real	NIFTI Node.sgauge. Limitor Resistance : Real	NIFTI Node.sgauge. Max input strain : Real	NIFTI Node.bmm. Battery State of Health : Real	NIFTI Node.sgauge. Current Drawn : electric current [ampere]
19	nifti node.sgauge2 : Quarter_Wheatstone_Bridge	500	500	50	0.05	0.8571	0.0113 A
20	nifti node.sgauge66 : Quarter_Wheatstone_Bridge	650	650	0	0.05	0.857	0.0112 A
21	nifti node.sgauge89 : Quarter_Wheatstone_Bridge	700	700	0	-0.05	0.8565	0.011 A
22	nifti node.sgauge25 : Quarter_Wheatstone_Bridge	550	550	50	-0.05	0.8564	0.0109 A
23	nifti node.sgauge486 : Full_Wheatstone_Bridge	550	550	50	0.05	0.8559	0.0107 A
24	nifti node.sgauge487 : Full_Wheatstone_Bridge	550	550	50	-0.05	0.8559	0.0107 A
25	nifti node.sgauge550 : Full_Wheatstone_Bridge	700	700	0	0.05	0.856	0.0107 A
26	nifti node.sgauge551 : Full_Wheatstone_Bridge	700	700	0	-0.05	0.856	0.0107 A
27	nifti node.sgauge24 : Quarter_Wheatstone_Bridge	550	550	50	0.05	0.8555	0.0105 A
28	nifti node.sgauge88 : Quarter_Wheatstone_Bridge	700	700	0	0.05	0.8554	0.0104 A
29	nifti node.sgauge111 : Quarter_Wheatstone_Bridge	750	750	0	-0.05	0.855	0.0103 A
30	nifti node.sgauge47 : Quarter_Wheatstone_Bridge	600	600	50	-0.05	0.8549	0.0102 A
31	nifti node.sgauge508 : Full_Wheatstone_Bridge	600	600	50	0.05	0.8545	0.01 A
32	nifti node.sgauge509 : Full_Wheatstone_Bridge	600	600	50	-0.05	0.8545	0.01 A
33	nifti node.sgauge572 : Full_Wheatstone_Bridge	750	750	0	0.05	0.8545	0.01 A
34	nifti node.sgauge573 : Full_Wheatstone_Bridge	750	750	0	-0.05	0.8545	0.01 A
35	nifti node.sgauge46 : Quarter_Wheatstone_Bridge	600	600	50	0.05	0.854	0.0098 A
36	nifti node.sgauge110 : Quarter_Wheatstone_Bridge	750	750	0	0.05	0.8539	0.0097 A
37	nifti node.sgauge133 : Quarter_Wheatstone_Bridge	800	800	0	-0.05	0.8537	0.0096 A
38	nifti node.sgauge69 : Quarter_Wheatstone_Bridge	650	650	50	-0.05	0.8535	0.0096 A
39	nifti node.sgauge5 : Quarter_Wheatstone_Bridge	500	500	100	-0.05	0.8534	0.0095 A
40	nifti node.sgauge466 : Full_Wheatstone_Bridge	500	500	100	0.05	0.853	0.0094 A
41	nifti node.sgauge467 : Full_Wheatstone_Bridge	500	500	100	-0.05	0.853	0.0094 A
42	nifti node.sgauge530 : Full_Wheatstone_Bridge	650	650	50	0.05	0.853	0.0094 A
43	nifti node.sgauge531 : Full_Wheatstone_Bridge	650	650	50	-0.05	0.853	0.0094 A
44	nifti node.sgauge594 : Full_Wheatstone_Bridge	800	800	0	0.05	0.853	0.0094 A
45	nifti node.sgauge595 : Full_Wheatstone_Bridge	800	800	0	-0.05	0.853	0.0094 A

Show Descripti

The table displays **924** of **924** total rows. **Status:**

Figure 9 Example inputs (e.g. Wheatstone Bridge types, Bridge and Strain Gauge Resistance, Limiting Resistor, Maximum Input Strain) and outputs (I_{Draw} and SOH) from multiple simulation runs

REFERENCES

Boyer P, Park S, Jerresand C, Sambath Ramkumar S, Balchanos MG, Pinon-Fischer OJ and Mavris D (2025) 'Design Environment for Lunar Operations and Systems Architecting', in AIAA SCITECH 2025 Forum, AIAA SciTech Forum, American Institute of Aeronautics and Astronautics, doi:10.2514/6.2025-0725.

INCOSE (2025) What is Systems Engineering, https://www.incose.org/about-systems-engineering/what-is-systems-engineering, accessed 15 August 2025.

LiPol Battery (2019) 'Lithium Polymer Battery Pack LP672030 350mAh 3.7V', https://www.lipolbattery.com/LiPo-Battery-Datahseet/LiPo_Battery_LP672030_3.7V_350mAh.pdf, accessed 15 August 2025.

Mancarella S (2025) 'A model-based systems engineering approach to deliver continued airworthiness through integrated working teams and datasets', AIAC 2025: 21st Australian International Aerospace Congress, Engineers Australia; Royal Aeronautical Society, Melbourne, https://search.informit.org/doi/10.3316/informit.T2025072500005700890708831, accessed 14 August 2025.

Mancarella S and Penhall P (2025) 'Insights from using a rapidly deployable, wireless data acquisition system for non-intrusive flight test instrumentation', AIAC 2025: 21st Australian International Aerospace Congress, Engineers Australia; Royal Aeronautical Society, Melbourne, https://search.informit.org/doi/10.3316/informit.T2025072500005891141430457, accessed 14 August 2025.

MEMKO (2025) 'NIFTI Application Guide - Sensor Harness Wiring for NIFTI Strain Gauge Sensor Node', https://nifti.aero/wp-content/uploads/2025/05/NIFTI-Application-Guide-Sensor-Harness-Wiring.pdf, accessed 15 August 2025.

Pattarakunnan K, Carta S and Penhall P (2025) 'Object-oriented modelling: A streamlined approach to simulate landing gear drop tests', AIAC 2025: 21st Australian International Aerospace Congress, Engineers Australia; Royal Aeronautical Society, Melbourne, https://search.informit.org/doi/10.3316/informit.T2025072500001891638259198, accessed 14 August 2025.

Schmalstieg J, Käbitz S, Ecker M and Sauer DU (2014) 'A holistic aging model for Li(NiMnCo)O2 based 18650 lithium-ion batteries', Journal of Power Sources, 257:325–334.

